ROYAL SOCIETY OF CHEMISTRY

PAPER

Check for updates

Assessing pH- and temperature-dependence in the aqueous phase partitioning of organic acids and bases in the atmosphere†

Olivia M. Driessen [ID] * and Jennifer G. Murphy [ID]

The gas-particle partitioning of low-volatility and semi-volatile organic compounds (L/S-VOCs) plays a dominant role in the formation of secondary organic aerosol, carrying implications for the health and climate effects of atmospheric particulate matter. Partitioning into aqueous particles and cloud droplets can also impact the fates of L/S-VOCs in the atmosphere. As the NH_3/NH_4^+ conjugate pair begins to dominate the buffering capacity of the atmospheric aqueous phase, there is a growing need to consider how changing particle acidity may impact the phase distribution of different ionizable compounds. In this work, we use a partitioning space framework and graphical assessment method to predict the effects of varied pH and temperature on the partitioning behavior of 24 ionizable organic compounds, including carboxylic acids and amines. As pH increases from 2 to 6, amines exhibit significantly increased affinity for the gas phase, whereas a preference for the aqueous phase is generated among several weak acids that would otherwise have remained vapors. We find that temperature can have a strong influence on the partitioning of some compounds. However, temperature-dependence can vary widely between compounds, and our analysis was limited by a lack of enthalpy values, necessitating reliable thermodynamic data for a larger number of L/S-VOCs. We implement a new visualization to investigate the partitioning behavior of lesser-studied compounds under varied conditions, and through this approach we see that aerosol liquid water content can greatly impact pH-sensitivity in partitioning.

Environmental significance

Understanding gas-particle partitioning is essential to our understanding of the composition and environmental impacts of particulate matter. Laboratory studies investigating secondary organic aerosol yield are often conducted under dry and/or warm conditions, with many lacking NH_3. However, in the environment, temperatures vary, particles may contain water, and NH_x species increasingly govern aerosol pH. In this work, we find that the partitioning of many ionizable organics is significantly impacted by varied pH and temperature, demonstrating the importance of considering their acid/base character in the atmosphere. The modelling approach used herein can be applied widely to predict the phase distribution of ionizable organics under various conditions, as well as to identify important variables and research gaps for future laboratory studies.

Introduction

Improved understanding of the composition and growth of atmospheric particulate matter (PM) is important for global climate and human health but faces challenges due to PM's chemical and physical complexity. Secondary PM, which can form through homogeneous nucleation from atmospheric gases as well as the condensation of gases on existing particles,[1] comprises a significant portion of the global aerosol budget.[2,3] The condensation of low-volatility and semi-volatile organic vapors, particularly the oxidation products of biogenic volatile

organic compounds (VOCs), is thought to dominate the growth of secondary organic aerosol (SOA).[1,4–6] Meanwhile, inorganic acids and bases, including sulfuric acid, nitric acid, and ammonia, have traditionally been recognized as the main drivers of particle nucleation, as well as the dominant components of aqueous aerosol.[7–10] However, studies in recent years have increasingly identified short-chain alkylamines as powerful agents in the formation of new particles,[11–13] as well as other small (C2 and C3) organics as constituents of aqueous SOA.[14] Understanding the gas-particle partitioning of low-volatility and semi-volatile organic compounds (L/S-VOCs) is critical, as organic compounds and their multiphase reactions can have major implications for aerosol physicochemical properties and climate forcing.[15,16]

Gas-particle partitioning of the compounds that contribute to SOA has often been modelled as a function of organic aerosol

Department of Chemistry, University of Toronto, 80 St. George Street, Toronto, ON M5S 3H6, Canada. E-mail: o.driessen@mail.utoronto.ca

† Electronic supplementary information (ESI) available. See DOI: https://doi.org/10.1039/d5ea00034c

© 2025 The Author(s). Published by the Royal Society of Chemistry

Environ. Sci.: Atmos., 2025, **5**, 591–602 | **591**

loading, temperature, and a compound's saturation vapor pressure, for example using the volatility basis set approach of Donahue et al.,[17] which treats PM as a single, organic condensed phase. However, aqueous solvation also plays an important role in the formation and chemical aging of SOA.[14,18] Recent observations of particle morphology demonstrate the occurrence of separate aqueous and organic phases within individual particles,[19–21] necessitating approaches that consider both phases simultaneously. The framework developed by Pankow[22] allows for the consideration of atmospheric liquid water, as well as acidic and basic species, in its modelling of equilibrium partitioning between gas and multi-phase PM. More recently, Wania et al.[23] introduced a two-dimensional chemical partitioning space to visualize the distribution of compounds between the gas, aqueous, and water-insoluble organic phases in the atmosphere. Their analysis of a selection of VOC oxidation products revealed the potential relevance of the aqueous phase for compounds not previously thought to be associated with aqueous SOA, including larger organics and many semi-volatile products of α-pinene. Particularly under conditions with high liquid water content (LWC), many S-VOCs which would otherwise remain vapors were predicted to contribute to SOA when partitioning to both the aqueous and organic phases was considered. The aerosol phase partitioning of organics can be impacted by not only the physicochemical properties of a given compound of interest, but additionally atmospheric conditions such as temperature, existing concentration of organic PM, relative humidity and the resultant aerosol LWC, and the inorganic electrolytes present in the PM.[1,20,24]

For ionizable organic compounds, pH can also have a strong influence on partitioning.[21,25] In the U.S. and Canada, the successful implementation of air quality regulations has led to significantly reduced emissions of SO_2 and NO_x in recent decades, but similar reductions have not been seen for NH_3 emissions.[26,27] As a result, Lawrence et al.[28] have observed long-term trends of decreased acidity in cloud water at Whiteface Mountain as the NH_3/NH_4^+ conjugate pair begins to dominate the buffer capacity of the atmospheric aqueous phase. Zheng et al.[29] also conclude that NH_x species control aerosol pH levels in many populated continental regions. In addition, the same group finds that aerosol systems in this NH_x-dominated regime are subject to increases or decreases in acidity over a wide range, with pH depending much more strongly on LWC as compared to sulfate-dominated systems.[29,30] Thus, the role of organics in aqueous PM may be evolving in recent years as the electrolyte composition changes. Current pH estimates based on field observations indicate wide ranges in atmospheric acidity, with aerosol pH ranging from −1 to 5, and cloud water pH from 2 to 7.[31,32] The influence of pH on partitioning in the indoor environment was recently demonstrated by Wang et al.,[33] who found that predicted gas-surface partitioning showed better agreement with observations when acid–base dissociation was taken into account. These findings imply a need for better understanding of the effects of NH_3 and pH changes on SOA composition and yield, especially given that chamber and flow reactor experiments investigating SOA yield are often conducted in dry air,[34–36] lack NH_3,[37–40] or both.[41–44] The effect of

temperature must also be considered, as most published studies are conducted at room temperature, leaving the cold conditions common to Earth's atmosphere underrepresented.[45] However, given the large number of variables impacting these systems, as well as the vast diversity of atmospheric compounds and reaction products that may contribute to SOA, it can be difficult to assess the relative importance of each variable for each specific case. Improved understanding of the compounds and conditions for which gas-particle partitioning could be sensitive to pH and temperature is needed. This will not only identify experimental research gaps, but will also provide insight into the environmental impacts of excess ammonia in the atmosphere.

In this study, we predict the effects of varied pH and temperature on the gas-particle partitioning behavior of 24 ionizable organic compounds, using the partitioning space framework of Wania et al.[23] and a combination of literature, computational, and experimentally derived thermodynamic parameters. We then introduce a modified graphical assessment method, based in the same thermodynamic principles, which can be used to evaluate pH-sensitivity in aqueous partitioning for a broad range of compounds and atmospheric conditions. Compounds of interest for our analysis comprise a range of atmospherically relevant organic acids and bases, including: low-molecular-weight amines, whose role in the enhancement of new particle formation is of great interest but whose gas phase concentrations are likely limited by their partitioning into existing aqueous particles;[11–13,46] monoprotic carboxylic acids that have been detected in PM and/or are known VOC oxidation products;[47–50] multiprotic carboxylic acids whose aqueous phase partitioning has been highlighted in recent studies and may be especially sensitive to ammonia's influence;[18,51–56] and organosulfates, significant acidic constituents of SOA whose thermodynamic properties are not well-known.[57–59]

Methods

In this work, we examine the partitioning of ionizable organic compounds between the gas (G), water (W), and water-insoluble organic matter (WIOM) phases in the atmosphere, using the two-dimensional partitioning space framework as defined by Wania et al.[23] The equilibrium partition coefficients, $K_{W/G}$ and $K_{WIOM/G}$, are predicted for each compound of interest from their physicochemical properties (equations outlined in ESI†). In order to investigate the effect of aerosol pH on partitioning behavior, $K_{W/G}$ is modified to incorporate the effective Henry's law constant, H_{eff}, calculated at a given pH and temperature for ionizable organics based on a compound's intrinsic H value and its pK_a value(s).

Through a combination of literature search, laboratory experiments, and prediction software, the necessary parameters were determined to examine the partitioning behavior of 24 ionizable organic compounds under varied aerosol pH. For seven of these compounds, enough data were available to model the effect of varied temperature on phase distribution (i.e., experimental enthalpy values associated with the Henry's Law

Table 1 Literature and estimated values of the pK_a, Henry's Law constant, vapor pressure, and respective enthalpies for the collection of atmospheric compounds studied in this work. For multiprotic compounds, data for all dissociations are reported in the same cell, separated by comma. Values confirmed to be experimentally determined are in bold type

Compound	pK_a	ΔH_{diss} (kJ mol^{-1})	H (M atm^{-1})	$\Delta H_{G \to w}$ (kJ mol^{-1})	p_L^0 (atm)	ΔH_{vap} (kJ mol^{-1})	References
Methylamine (MA)	10.660	54.737	35	−22	3.32	23.61	46 and 60–62
Dimethylamine (DMA)	10.730	49.45	30.3	−30	1.9	25.44	46 and 60–62
	—	50.8	—	—	—	—	63
Trimethylamine (TMA)	9.800	36.017	9.63	—	2.28	22.18	46, 60 and 62
Ethanolamine (MEA)	**9.49**	50.80	**6.1×10^6**	—	6.415×10^{-4}	59.63	62 and 64–66
	9.45	**48.05**	—	—	—	—	67
	—	48.72	—	—	—	—	68
	9.50	50.61	—	—	—	—	46 and 60
Putrescine (PS)	10.80, 9.63	—	2.86×10^6	—	3.06×10^{-3}	—	60, 69 and 70
	—	—	—	—	5.42×10^{-3}	—	71
Cadaverine (CV)	10.05, 10.93	—	2.04×10^6	—	1.33×10^{-3}	—	60, 69 and 70
Urea (UR)	0.10	—	5.8×10^8	—	1.5×10^{-8}	—	60 and 72
Trifluoroacetic acid (TFA)	0.47	**1.67**	**5780**	**−34.2**	0.153	33.3	50, 60, 73 and 74
	—	—	**8950**	**−77.6**	—	—	50
Oxalic acid (OA)	**1.2, 3.85**	**−3.27, 6.20**	7.2×10^8	−81	**2.9×10^{-7}**	79	75–77
	1.25	3.81	6.2×10^8	−61	—	—	60, 78 and 79
Adipic acid (AA)	4.41^a, 5.41^a	**12.91, −18.34**	6.7×10^9	−110	**9.7×10^{-11}**	**154**	60, 78, 80 and 81
	—	—	1.8×10^7	−91	—	—	62
	—	—	2.1×10^8	—	—	—	72
Phthalic acid (PhA)	2.943, 5.432	**−19.49, −8.16**	5.0×10^7	—	**8.37×10^{-10}**	**407.8**	60, 72, 82 and 83
Glutaric acid (GA)	4.32^a, 5.42	—	5.2×10^9	−100	**1.11×10^{-8}**	**100.8**	60, 78 and 84
2-Hydroxyisobutyric acid (HIBA)	3.96	—	9.09×10^5	—	1.7×10^{-5}	55.02	85, italicized values predicted in this work using SPARC^b
Pyruvic acid (PyA)	2.38	—	**3.11×10^5**	−42.3	1.7×10^{-3}	**53.6**	60, 71, 86 and 87
Pinic acid (PiA)	**4.24, 5.40**	—	1.04×10^9	—	**4.308×10^{-10}**	**109**	88 and 89, italicized values predicted in this work using SPARC^b
cis-Pinonic acid (CPA)	**4.48, 5.48**	—	—	—	—	—	90
	4.82	—	6.10×10^6	—	2.34×10^{-8}	111.8	90, italicized values predicted in this work using SPARC^b
	5.19	—	—	—	—	—	91
Malonic acid (MaA)	2.85, 5.7	—	3.9×10^{10}	−92	**4.2×10^{-9}**	**96**	60, 77 and 78
Succinic acid (SA)	4.21, 5.64	3.0, −0.5	4.2×10^9	−94	**1.7×10^{-8}**	**106**	60, 77, 78 and 92
Lactic acid (LA)	3.86	—	1.2×10^4	—	1.07×10^{-4}	**69.1**	72, 93 and 94
Levulinic acid (LV)	4.78	—	1.02×10^7	—	**5.23×10^{-6}**	74.4	95–97, italicized values predicted in this work using SPARC^b
Glycolic acid (GcA)	3.83	—	**2.34×10^4**	**−33.5**	2.6×10^{-5}	51.8	71, 72, 97 and 98
4-Methyl-2-oxovaleric acid (MOVA)	*3.60*	—	*735*	—	*2.1×10^{-4}*	*67.53*	Predicted in this work using SPARC^b
3-Methyl-1,2,3-butanetricarboxylic acid (MBTCA)	**3.62, 4.97, 6.80**	—	1.92×10^{10}	—	**1.4×10^{-11}**	—	88 and 99
2-Methyltetrol sulfate^c (MTS)	*0.48*	—	*1.86×10^{12}*	—	*2.95×10^{-11}*	*154*	Predicted in this work using SPARC^b

^{a} pK_a at 18 °C. ^{b} SPARC Performs Automated Reasoning in Chemistry,[100] calculation specifications described in main text. ^{c} General structure, no stereochemistry.

© 2025 The Author(s). Published by the Royal Society of Chemistry

Environ. Sci.: Atmos., 2025, **5**, 591–602 | **593**

Table 2 Experimentally determined enthalpies of dissociation, compared to literature values where available

Compound	Experimental ΔH_{diss} (kJ mol^{-1})	Literature ΔH_{diss} (kJ mol^{-1})	References
Ammonia	53 ± 3	51.92	101 (Experimental)
Methylamine	52 ± 3	54.737	46 (Computed)
Ethanolamine	42 ± 2	48.05	67 (Experimental)
cis-Pinonic acid	−7.0 ± 0.4		
2-Hydroxyisobutyric acid	5 ± 5		

constant, acid/base dissociation, and vaporization). Table 1 contains the relevant physicochemical parameters available for the compounds investigated in this work.

Experimental and computational estimation of parameters

For many atmospherically relevant molecules, experimental values for each of the thermodynamic parameters are not available in the literature. In this work, the enthalpies of dissociation of two organic acids (*cis*-pinonic acid (CPA) and 2-hydroxyisobutyric acid (HIBA)) were determined for the first time that we know of *via* temperature-controlled potentiometric titrations, which was also applied to ammonia, and two amines (MA and MEA). At temperatures in the range of 2–45 °C, solutions of the analytes at 0.015 M were titrated with either HCl or NaOH at 0.3 M, and pH and temperature measurements were conducted using a calibrated HACH sensION™ electrode. Temperature was controlled using a refrigerated circulating bath, filled with aqueous ethylene glycol solution and connected to the half-jacketed flask that was the titration vessel. The pK_a value at each temperature was determined from the first derivative of the titration curve, and dissociation enthalpies were derived from the resultant van't Hoff curves, with each uncertainty calculated from the standard error in the slope (Table 2). Our experimental dissociation enthalpy values show reasonable agreement with the available literature values, and experimental ambient-temperature pK_a values (measured at approximately 20 °C) all fell within 0.3 units of the corresponding room-temperature literature values (Table S1†).

Finally, for several lesser-studied compounds, values of the Henry's Law constant, pK_a, vapor pressure, and/or enthalpy of vaporization, were estimated using SPARC Performs Automated Reasoning in Chemistry (SPARC).[100] This calculation package outputs various physicochemical parameters based on the chemical structure of a compound, directly from the input of a SMILES code. For this work, calculations were carried out for a temperature of 25 °C and a pressure of 1 atm. For vapor pressure calculations, which require the input of the compound's melting point, either the SPARC-suggested melting point was used, or the compound was assumed to be liquid at room temperature. Values predicted for this work using SPARC are shown italicized in Table 1.

Results and discussion

Based on their estimated $K_{W/G}$ and $K_{WIOM/G}$, each compound of interest is placed in the two-dimensional partitioning space, where its affinity for the gas, aqueous, or WIOM phase may be assessed under specified atmospheric conditions. The phase boundaries in Fig. 1 and 2 are drawn for a model case of urban PM$_{2.5}$,[16,102] where liquid water content (LWC) and organic aerosol loading (OAL) are both 10 μg m^{-3}, the density of both phases is assumed to be 10^6 g m^{-3}, and the temperature is 298.15 K. For all figures, an average molecular weight of the WIOM, 240 g mol^{-1}, is used to calculate the gas-particle partition coefficient, K',[22,103] which is incorporated into $K_{WIOM/G}$. For this study, we assumed ideal mixing in each phase.

Comparing the panels of Fig. 1, we see that the modeled aqueous phase affinity of several compounds is noticeably altered when taking ionizability into account through the use of H_{eff}. As pH increases from 2 to 6 (Fig. 1B–D), the amines exhibit decreased affinity for the aqueous phase, whereas weak organic acids are predicted to partition more significantly into aqueous aerosol.

Where all necessary enthalpy values are available, the effects of varied temperature on partitioning may be investigated as well. In Fig. 2, the combined trends with pH and temperature are shown for seven compounds for which the relevant enthalpy values are known. Among the amines, there are steep slopes in temperature dependence, indicating that temperature may exert significant influence on their partitioning between gas and aqueous aerosol. This can be attributed to the strong temperature dependence of their dissociation constant, which impacts H_{eff}, as well as the relatively weaker temperature dependence of the intrinsic H and p_L^0 values (Table 1). For the acids, the enthalpies of vaporization are larger in magnitude than those of the amines, leading to a comparable or even greater influence of temperature on $K_{WIOM/G}$ than on $K_{W/G}$. Temperature dependence curves have only been added to the plot at pH 6 to preserve the readability of Fig. 2, but it should be noted that differences in temperature dependence may be observed between pH values for multiprotic compounds, as each dissociation is associated with a distinct enthalpy value. For the multiprotic acids analyzed in this study, these differences were small enough as to not be visually distinguishable in the figure, due to the weak temperature-dependence in the dissociation of these compounds.

The established framework can then be recast to probe the pH-sensitivity of the partitioning behavior of a wider range of compounds for which complete and reliable thermodynamic data is not available. Rearrangement of the equation for the aqueous phase fraction as presented by Wania *et al.*[23] and that of H_{eff} allows for the determination of the pH–pK_a difference required for a monoprotic compound to partition into the aqueous phase to a given degree, under a specified set of aerosol
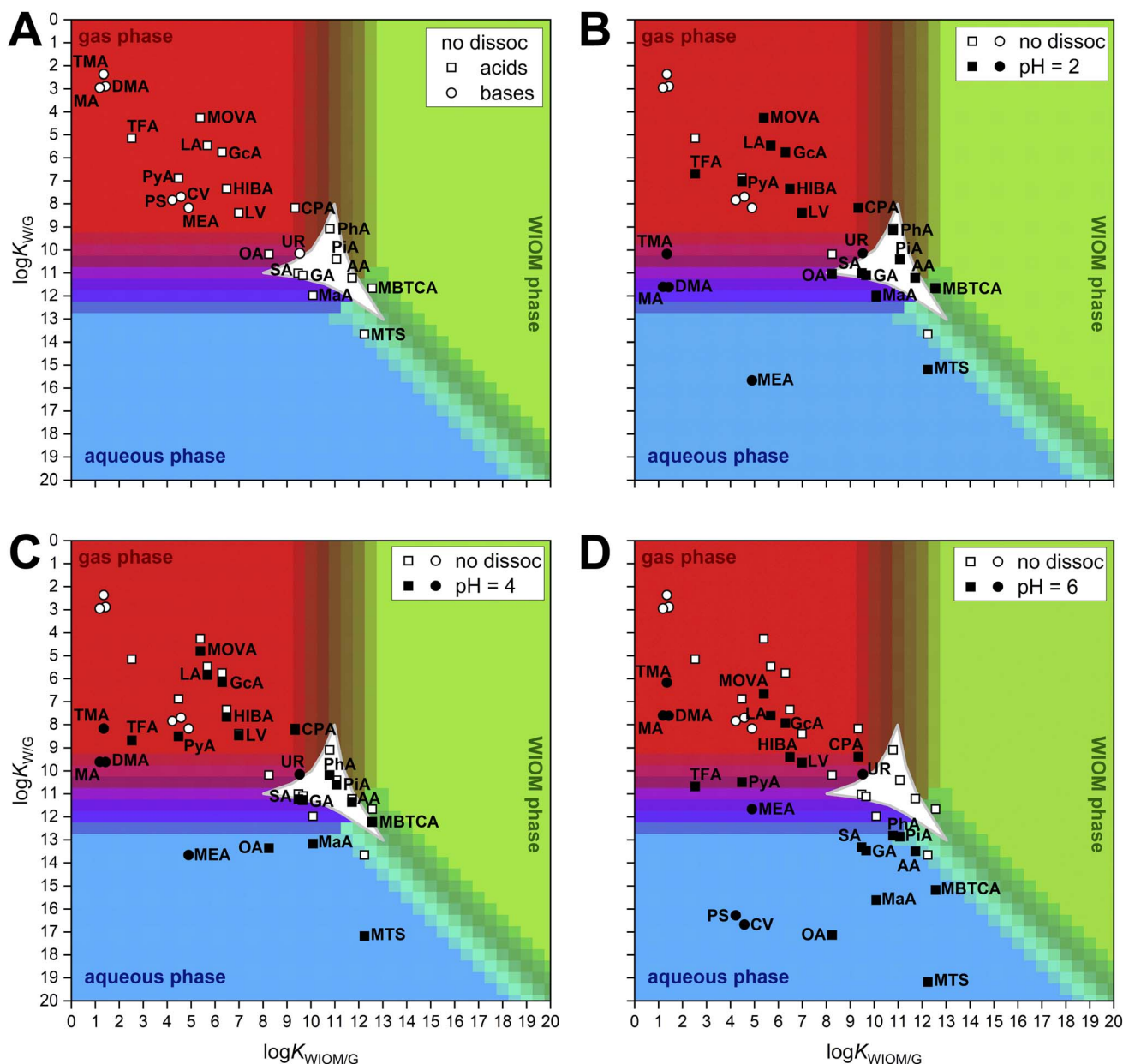
Fig. 1 Placement of ionizable organic compounds in the atmospheric chemical partitioning space. $K_{W/G}$ and $K_{WIOM/G}$ values are calculated from thermodynamic properties at 25 °C, for a model case where LWC = OAL = 10 μg m^{-3}. Panel (A) ignores acid–base dissociation and assumes all compounds are fully comprised of the neutral species, while panels (B–D) consider speciation at pH 2, 4, and 6, respectively, using the H_{eff} to derive $K_{W/G}$.

conditions (equation shown in ESI†). The requisite difference between pH and pK_a is visualized as a function of the compound's intrinsic H and p_L^0 values. In Fig. 3A, we identify the pH–pK_a difference at which each compound's aqueous phase partitioning is most sensitive to changing aerosol conditions (50% aqueous phase fraction), under a model case for urban PM$_{2.5}$.

For the range of monoprotic compounds studied here (with pure liquid vapor pressures of $\sim$10^{-6}–10^6 Pa), vapor pressure does not appear to have an appreciable influence on the pH-sensitivity of their partitioning under the given conditions. However, as can be seen from the change in shading on the far-

left side of Fig. 3A, pH-sensitivity in partitioning (at a constant value of H) begins to decrease as vapor pressure decreases below $\sim$10^{-8} Pa in this system, corresponding to compounds that show strong intrinsic affinity for the WIOM phase (log $K_{WIOM/G}$ values > 14). The interplay of aqueous-phase pH effects with compound vapor pressure would also likely be more significant in systems with higher OAL.

The relationship between H, p_L^0, and pH-sensitivity is expected to be strongly influenced by LWC for many compounds of interest. Fig. 3B uses a model case of cloud droplets,[104] with LWC = 140 mg m^{-3}. In this case, a much lower pH–pK_a difference is required to generate a preference for the aqueous

© 2025 The Author(s). Published by the Royal Society of Chemistry

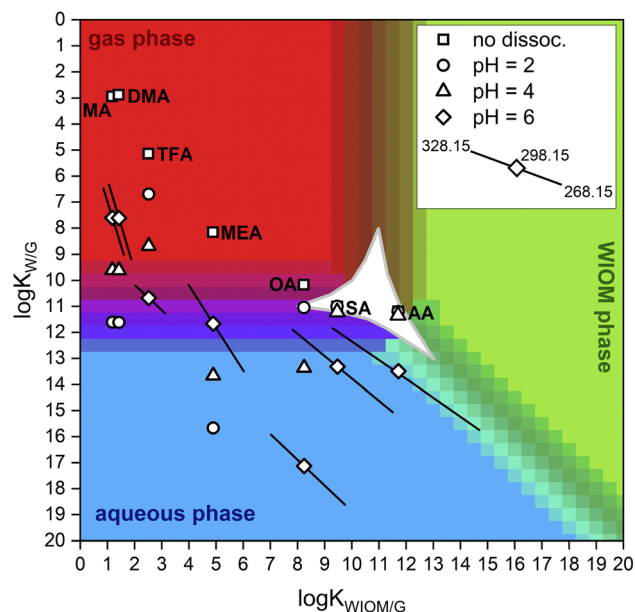*Environ. Sci.: Atmos.*, 2025, **5**, 591–602 | **595**

Fig. 2 Partitioning space placement of all compounds of interest for which dissociation, aqueous solvation, and vaporization enthalpy values were available in the literature. Placements of the fully neutral compounds (labeled) are in vertical alignment with their respective pH-impacted placements. Trends in varied temperature are displayed at pH 6.

phase for all compounds studied, and a compound's p_L^0 exerts even less influence than in the case of LWC = 10 μg m^{-3}.

The visualization shown in Fig. 3 can be used for a detailed projection of which phase will dominate the fate of individual

compounds of atmospheric interest under different sets of conditions. For instance, with DMA, whose pK_a is 10.73,[60] preference for the aqueous phase in our urban PM$_{2.5}$ model case would require a highly acidic aerosol pH, no greater than 2–3. However, in our cloud droplet system, anything below an approximately neutral pH would result in a preference for the aqueous phase by DMA. Meanwhile, the pH of urban PM$_{2.5}$ would need to be approximately neutral or above for TFA (pK_a = 0.47)[50] to preferentially partition into the aqueous phase, but any pH above 2–2.5 would result in over 50% abundance of TFA in aqueous cloud droplets. This analysis can also be applied to lesser-studied compounds for which the pK_a is not known, such as organosulfates. Using H and p_L^0 values estimated in SPARC based on chemical structure, we see that the organosulfate MTS likely shows a strong preference for the aqueous aerosol phase regardless of pH and LWC.

Although much of this study has focused on small organic acids and bases whose aqueous affinity is primarily in competition with the gas phase, larger, more "WIOM-like" organic molecules are also significant atmospheric constituents, and long-chain n-alkanoic acids have been detected in PM, due to diesel vehicle emissions,[105] as well as originating from plant wax.[106] Our graphical assessment approach facilitates a low-effort examination of whether these compounds' partitioning behavior warrants a closer look with regard to variation in pH. We find that the partitioning behavior of long-chain n-alkanoic acids (C15–C23) would likely not be sensitive to pH changes in PM with low LWC. Despite the apparent change in pH-sensitivity between the two panels of Fig. 3, these compounds are realistically not much more likely to partition into cloud water than into aqueous PM, as they still require a pH–pK_a
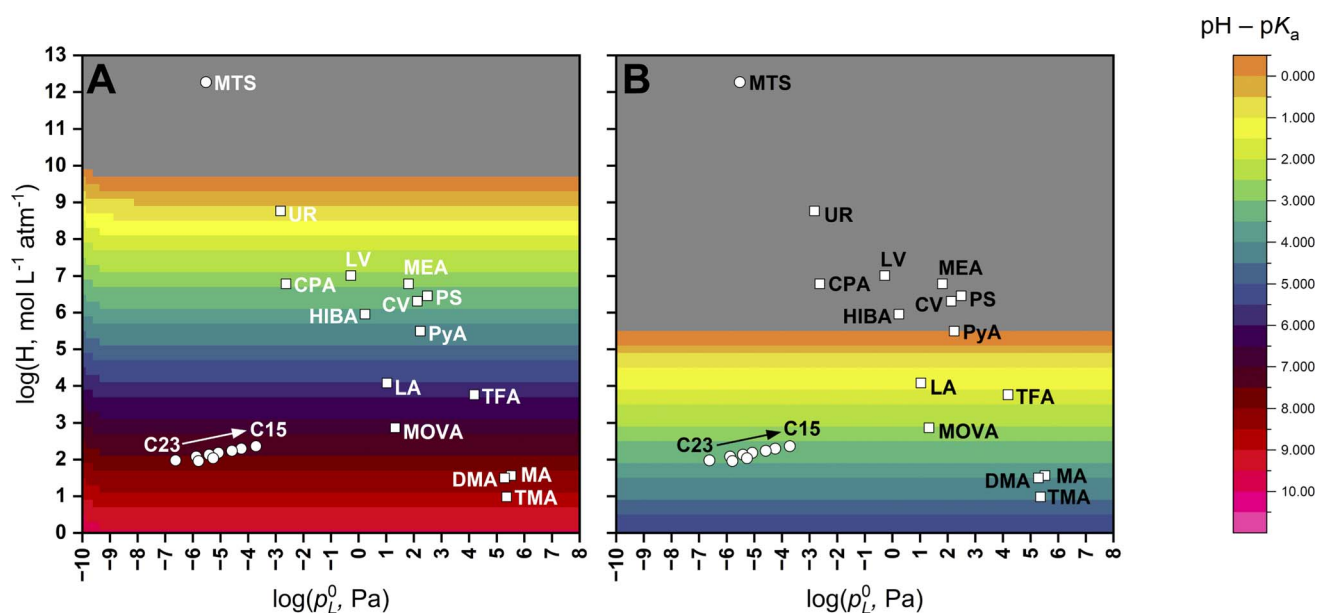

Fig. 3 Monoprotic compounds of interest placed in pH-sensitivity assessment plot, where shading represents the absolute value of the minimum pH–pK_a difference required for a compound with a given H and p_L^0 to partition 50% into the aqueous aerosol phase at 25 °C. Compounds whose dominant reservoir is the gas phase are represented by square symbols, whereas circles represent compounds with a preference for the WIOM phase over the gas phase. (A) Urban PM$_{2.5}$ model case, where LWC = OAL = 10 μg m^{-3}. (B) Cloud model case, where LWC = 140 mg m^{-3}, and OAL = 10 μg m^{-3}.

596 | *Environ. Sci.: Atmos.*, 2025, **5**, 591–602

© 2025 The Author(s). Published by the Royal Society of Chemistry

difference of 3–3.5 for a 50% fraction in the aqueous phase relative to the WIOM phase. The pK_a values of these large organic acids are likely to be greater than 5, based on the longest-chain acid for which literature data is available (dodecanoic acid, pK_a = 5.3 at 20 °C).[72]

Overall, the results of these analyses indicate that the aqueous phase affinity of ionizable compounds can be highly sensitive to changes in pH. This has implications for the composition and resultant properties of aerosol and cloud water in the environment. In addition, we find that ionizable organics may exhibit widely varying temperature dependence in their gas-particle partitioning, particularly when considering all three phases. The amines studied herein, which have large dissociation enthalpy values, show a strong temperature dependence in their aqueous partitioning. Meanwhile, the organic acids we have studied tend to show comparable or stronger temperature dependence in their partitioning into the WIOM phase. Finally, we have implemented a graphical pH-sensitivity assessment approach, which can be used to forecast the importance of the aqueous phase for a wide variety of compounds under specified atmospheric conditions. We find that the relationship between H, p_L^0, and pH-sensitivity in aqueous partitioning is strongly dependent on aerosol conditions such as LWC and OAL. Although the WIOM phase is not predicted to be a dominant reservoir for many of the compounds and model systems studied herein, WIOM-W phase partitioning, as well as p_L^0, may play a more significant role for larger, lower-volatility organic compounds, or in systems with a higher organic aerosol loading.

Conclusion

This work demonstrates the importance of considering the effect of pH on the gas-particle partitioning of ionizable organics, particularly given the wide pH-variation and changing composition observed in the atmospheric aqueous phase. In regions where a long-term increase in aerosol pH is observed, weak bases like amines may show increased abundance in the gas phase, potentially influencing their relevance for new particle formation. Meanwhile, decreased PM acidity could increase the aqueous-phase abundance of many organic acids which may otherwise have remained vapors. Opposite trends could be observed in regions with increased aerosol acidity. These changes in PM composition, and in turn, related multiphase reaction pathways, could impact the optical properties of aerosols and their effects on human health, as well as the fates of various atmospheric pollutants. Accurately predicting gas-particle partitioning with these processes in mind, using the techniques shown herein, will improve our understanding of the health and climate effects of PM.

While we found that temperature can have a strong influence on the partitioning behavior of some atmospheric species, our temperature-dependence analysis was limited to compounds with complete, reliable thermodynamic data available, which is not the case for the vast majority of compounds relevant to SOA. Experimental data are generally preferable with regard to enthalpy values, as there can be wide discrepancies when using computational estimation techniques.[107–109] Enthalpy values for vaporization, aqueous solvation, and dissociation should be experimentally determined for more analytes, but given the immense number of atmospherically relevant compounds, this poses a challenge for investigating temperature dependence in partitioning at present. The graphical pH-sensitivity assessment approach implemented in this work helps address that challenge. This technique is useful for predicting the fate of compounds whose properties are not well-studied, as it utilizes only two compound-specific parameters, which for these purposes can be experimental or computational values. The prediction of pH-sensitivity in partitioning can inform laboratory studies by indicating the importance of variables such as humidity and inorganic content in SOA, as well as identifying compounds for which more thermodynamic data is needed.

Data availability

All data supporting this article have been included as part of the main text or ESI.†

Author contributions

Conceptualization, project administration, and writing – review & editing: all authors; data curation, formal analysis, investigation, visualization, writing – original draft: O. M. D.; funding acquisition, resources, supervision: J. G. M.
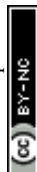
Conflicts of interest

There are no conflicts to declare.

Acknowledgements

References

1 J. H. Seinfeld and J. F. Pankow, Organic Atmospheric Particulate Material, *Annu. Rev. Phys. Chem.*, 2003, **54**, 121–140.
2 D. V Spracklen, K. S. Carslaw, M. Kulmala, V.-M. Kerminen, G. W. Mann and S.-L. Sihto, The contribution of boundary layer nucleation events to total particle concentrations on regional and global scales, *Atmos. Chem. Phys.*, 2006, **6**, 5631–5648.
3 D. V. Spracklen, K. S. Carslaw, J. Merikanto, G. W. Mann, C. L. Reddington, S. Pickering, J. A. Ogren, E. Andrews, U. Baltensperger, E. Weingartner, M. Boy, M. Kulmala, L. Laakso, H. Lihavainen, N. Kivekäs, M. Komppula, N. Mihalopoulos, G. Kouvarakis, S. G. Jennings, C. O'Dowd, W. Birmili, A. Wiedensohler, R. Weller, J. Gras, P. Laj, K. Sellegri, B. Bonn, R. Krejci, A. Laaksonen, A. Hamed, A. Minikin, R. M. Harrison, R. Talbot and J. Sun, Explaining global surface aerosol number concentrations in terms of primary emissions

© 2025 The Author(s). Published by the Royal Society of Chemistry

Environ. Sci.: Atmos., 2025, **5**, 591–602 | **597**

and particle formation, *Atmos. Chem. Phys.*, 2010, **10**, 4775–4793.

4 I. Riipinen, T. Yli-Juuti, J. R. Pierce, T. Petäjä, D. R. Worsnop, M. Kulmala and N. M. Donahue, The contribution of organics to atmospheric nanoparticle growth, *Nat. Geosci.*, 2012, **5**, 453–458.

5 M. Ehn, J. A. Thornton, E. Kleist, M. Sipilä, H. Junninen, I. Pullinen, M. Springer, F. Rubach, R. Tillmann, B. Lee, F. Lopez-Hilfiker, S. Andres, I.-H. Acir, M. Rissanen, T. Jokinen, S. Schobesberger, J. Kangasluoma, J. Kontkanen, T. Nieminen, T. Kurtén, L. B. Nielsen, S. Jørgensen, H. G. Kjaergaard, M. Canagaratna, M. D. Maso, T. Berndt, T. Petäjä, A. Wahner, V.-M. Kerminen, M. Kulmala, D. R. Worsnop, J. Wildt and T. F. Mentel, A large source of low-volatility secondary organic aerosol, *Nature*, 2014, **506**, 476–479.

6 M. Claeys, B. Graham, G. Vas, W. Wang, R. Vermeylen, V. Pashynska, J. Cafmeyer, P. Guyon, M. O. Andreae, P. Artaxo and W. Maenhaut, Formation of Secondary Organic Aerosols Through Photooxidation of Isoprene, *Science*, 2004, **303**, 1173–1176.

7 J. Kirkby, J. Curtius, J. Almeida, E. Dunne, J. Duplissy, S. Ehrhart, A. Franchin, S. Gagné, L. Ickes, A. Kürten, A. Kupc, A. Metzger, F. Riccobono, L. Rondo, S. Schobesberger, G. Tsagkogeorgas, D. Wimmer, A. Amorim, F. Bianchi, M. Breitenlechner, A. David, J. Dommen, A. Downard, M. Ehn, R. C. Flagan, S. Haider, A. Hansel, D. Hauser, W. Jud, H. Junninen, F. Kreissl, A. Kvashin, A. Laaksonen, K. Lehtipalo, J. Lima, E. R. Lovejoy, V. Makhmutov, S. Mathot, J. Mikkilä, P. Minginette, S. Mogo, T. Nieminen, A. Onnela, P. Pereira, T. Petäjä, R. Schnitzhofer, J. H. Seinfeld, M. Sipilä, Y. Stozhkov, F. Stratmann, A. Tomé, J. Vanhanen, Y. Viisanen, A. Vrtala, P. E. Wagner, H. Walther, E. Weingartner, H. Wex, P. M. Winkler, K. S. Carslaw, D. R. Worsnop, U. Baltensperger and M. Kulmala, Role of sulphuric acid, ammonia and galactic cosmic rays in atmospheric aerosol nucleation, *Nature*, 2011, **476**, 429–433.

8 Y. Wang, G. Zhuang, X. Zhang, K. Huang, C. Xu, A. Tang, J. Chen and Z. An, The ion chemistry, seasonal cycle, and sources of PM2.5 and TSP aerosol in Shanghai, *Atmos. Environ.*, 2006, **40**, 2935–2952.

9 C.-M. Kang, H. S. Lee, B.-W. Kang, S.-K. Lee and Y. Sunwoo, Chemical characteristics of acidic gas pollutants and PM2.5 species during hazy episodes in Seoul, South Korea, *Atmos. Environ.*, 2004, **38**, 4749–4760.

10 S. T. Martin, Phase Transitions of Aqueous Atmospheric Particles, *Chem. Rev.*, 2000, **100**, 3403–3454.

11 A. Kürten, C. Li, F. Bianchi, J. Curtius, A. Dias, N. M. Donahue, J. Duplissy, R. C. Flagan, J. Hakala, T. Jokinen, J. Kirkby, M. Kulmala, A. Laaksonen, K. Lehtipalo, V. Makhmutov, A. Onnela, M. P. Rissanen, M. Simon, M. Sipilä, Y. Stozhkov, J. Tröstl, P. Ye and P. H. McMurry, New particle formation in the sulfuric acid–dimethylamine–water system: reevaluation of CLOUD chamber measurements and comparison to an aerosol nucleation and growth model, *Atmos. Chem. Phys.*, 2018, **18**, 845–863.

12 M. E. Erupe, A. A. Viggiano and S.-H. Lee, The effect of trimethylamine on atmospheric nucleation involving H<sub>2</sub>SO<sub>4</sub>, *Atmos. Chem. Phys.*, 2011, **11**, 4767–4775.

13 T. Berndt, F. Stratmann, M. Sipilä, J. Vanhanen, T. Petäjä, J. Mikkilä, A. Grüner, G. Spindler, R. Lee Mauldin III, J. Curtius, M. Kulmala and J. Heintzenberg, Laboratory study on new particle formation from the reaction OH + SO<sub>2</sub>: influence of experimental conditions, H<sub>2</sub>O vapour, NH<sub>3</sub> and the amine tert-butylamine on the overall process, *Atmos. Chem. Phys.*, 2010, **10**, 7101–7116.

14 Y. B. Lim, Y. Tan, M. J. Perri, S. P. Seitzinger and B. J. Turpin, Aqueous chemistry and its role in secondary organic aerosol (SOA) formation, *Atmos. Chem. Phys.*, 2010, **10**, 10521–10539.

15 S. F. Maria, L. M. Russell, M. K. Gilles and S. C. B. Myneni, Organic Aerosol Growth Mechanisms and Their Climate-Forcing Implications, *Science*, 2004, **306**, 1921–1924.

16 J. L. Jimenez, M. R. Canagaratna, N. M. Donahue, A. S. H. Prevot, Q. Zhang, J. H. Kroll, P. F. DeCarlo, J. D. Allan, H. Coe, N. L. Ng, A. C. Aiken, K. S. Docherty, I. M. Ulbrich, A. P. Grieshop, A. L. Robinson, J. Duplissy, J. D. Smith, K. R. Wilson, V. A. Lanz, C. Hueglin, Y. L. Sun, J. Tian, A. Laaksonen, T. Raatikainen, J. Rautiainen, P. Vaattovaara, M. Ehn, M. Kulmala, J. M. Tomlinson, D. R. Collins, M. J. Cubison, J. Dunlea, J. A. Huffman, T. B. Onasch, M. R. Alfarra, P. I. Williams, K. Bower, Y. Kondo, J. Schneider, F. Drewnick, S. Borrmann, S. Weimer, K. Demerjian, D. Salcedo, L. Cottrell, R. Griffin, A. Takami, T. Miyoshi, S. Hatakeyama, A. Shimono, J. Y. Sun, Y. M. Zhang, K. Dzepina, J. R. Kimmel, D. Sueper, J. T. Jayne, S. C. Herndon, A. M. Trimborn, L. R. Williams, E. C. Wood, A. M. Middlebrook, C. E. Kolb, U. Baltensperger and D. R. Worsnop, Evolution of Organic Aerosols in the Atmosphere, *Science*, 2009, **326**, 1525–1529.

17 N. M. Donahue, A. L. Robinson, C. O. Stanier and S. N. Pandis, Coupled partitioning, dilution, and chemical aging of semivolatile organics, *Environ. Sci. Technol.*, 2006, **40**, 2635–2643.

18 M. N. Chan, H. Zhang, A. H. Goldstein and K. R. Wilson, Role of Water and Phase in the Heterogeneous Oxidation of Solid and Aqueous Succinic Acid Aerosol by Hydroxyl Radicals, *J. Phys. Chem. C*, 2014, **118**, 28978–28992.

19 A. Zuend and J. H. Seinfeld, Modeling the gas-particle partitioning of secondary organic aerosol: The importance of liquid-liquid phase separation, *Atmos. Chem. Phys.*, 2012, **12**, 3857–3882.

20 M. Shiraiwa, A. Zuend, A. K. Bertram and J. H. Seinfeld, Gas-particle partitioning of atmospheric aerosols: Interplay of physical state, non-ideal mixing and morphology, *Phys. Chem. Chem. Phys.*, 2013, **15**, 11441–11453.

21 J. F. Pankow, Phase considerations in the gas/particle partitioning of organic amines in the atmosphere, *Atmos. Environ.*, 2015, **122**, 448–453.

22 J. F. Pankow, Gas/particle partitioning of neutral and ionizing compounds to single and multi-phase aerosol particles. 1. Unified modeling framework, *Atmos. Environ.*, 2003, **37**, 3323–3333.

23 F. Wania, Y. D. Lei, C. Wang, J. P. D. Abbatt and K. U. Goss, Using the chemical equilibrium partitioning space to explore factors influencing the phase distribution of compounds involved in secondary organic aerosol formation, *Atmos. Chem. Phys.*, 2015, **15**, 3395–3412.

24 M. Hallquist, J. C. Wenger, U. Baltensperger, Y. Rudich, D. Simpson, M. Claeys, J. Dommen, N. M. Donahue, C. George, A. H. Goldstein, J. F. Hamilton, H. Herrmann, T. Hoffmann, Y. Iinuma, M. Jang, M. E. Jenkin, J. L. Jimenez, A. Kiendler-Scharr, W. Maenhaut, G. Mcfiggans, T. F. Mentel, A. Monod, A. S. H. Prévôt, J. H. Seinfeld, J. D. Surratt, R. Szmigielski and J. Wildt, *The Formation, Properties and Impact of Secondary Organic Aerosol: Current and Emerging Issues*, 2009, vol. 9.

25 A. Tilgner, T. Schaefer, B. Alexander, M. Barth, J. L. Collett Jr, K. M. Fahey, A. Nenes, H. O. T. Pye, H. Herrmann and V. F. McNeill, Acidity and the multiphase chemistry of atmospheric aqueous particles and clouds, *Atmos. Chem. Phys.*, 2021, **21**, 13483–13536.

26 EPA's 2020, *National Emissions Inventory and Trends Report*, 2023.

27 National Pollutant Release Inventory: sulphur dioxide, https://www.canada.ca/en/environment-climate-change/ services/national-pollutant-release-inventory/tools- resources-data/sulphur-dioxide.html, accessed 24 June 2024.

28 C. E. Lawrence, P. Casson, R. Brandt, J. J. Schwab, J. E. Dukett, P. Snyder, E. Yerger, D. Kelting, T. C. Vandenboer and S. Lance, Long-term monitoring of cloud water chemistry at Whiteface Mountain: The emergence of a new chemical regime, *Atmos. Chem. Phys.*, 2023, **23**, 1619–1639.

29 G. Zheng, H. Su, S. Wang, M. O. Andreae, U. Pöschl and Y. Cheng, Multiphase buffer theory explains contrasts in atmospheric aerosol acidity, *Science*, 2020, **369**, 1374–1377.

30 G. Zheng, H. Su, R. Wan, X. Duan and Y. Cheng, Rising Alkali-to-Acid Ratios in the Atmosphere May Correspond to Increased Aerosol Acidity, *Environ. Sci. Technol.*, 2024, **58**, 16517–16524.

31 H. O. T. Pye, A. Nenes, B. Alexander, A. P. Ault, M. C. Barth, S. L. Clegg, J. L. Collett Jr, K. M. Fahey, C. J. Hennigan, H. Herrmann, M. Kanakidou, J. T. Kelly, I.-T. Ku, V. F. McNeill, N. Riemer, T. Schaefer, G. Shi, A. Tilgner, J. T. Walker, T. Wang, R. Weber, J. Xing, R. A. Zaveri and A. Zuend, The acidity of atmospheric particles and clouds, *Atmos. Chem. Phys.*, 2020, **20**, 4809–4888.

32 A. P. Ault, Aerosol Acidity: Novel Measurements and Implications for Atmospheric Chemistry, *Acc. Chem. Res.*, 2020, **53**, 1703–1714.

33 C. Wang, D. B. Collins, C. Arata, A. H. Goldstein, J. M. Mattila, D. K. Farmer, L. Ampollini, P. F. Decarlo, A. Novoselac, M. E. Vance, W. W. Nazaroff and J. P. D. Abbatt, *Surface Reservoirs Dominate Dynamic Gas-Surface Partitioning of Many Indoor Air Constituents*, 2020, vol. 6.

34 J. E. Shilling, Q. Chen, S. M. King, T. Rosenoern, J. H. Kroll, D. R. Worsnop, K. A. McKinney and S. T. Martin, Particle mass yield in secondary organic aerosol formed by the dark ozonolysis of α-pinene, *Atmos. Chem. Phys.*, 2008, **8**, 2073–2088.

35 R. K. Pathak, C. O. Stanier, N. M. Donahue and S. N. Pandis, Ozonolysis of α -pinene at atmospherically relevant concentrations: Temperature dependence of aerosol mass fractions (yields), *J. Geophys. Res.:Atmos.*, 2007, **112**, D03201.

36 N. L. Ng, J. H. Kroll, M. D. Keywood, R. Bahreini, V. Varutbangkul, R. C. Flagan, J. H. Seinfeld, A. Lee and A. H. Goldstein, Contribution of First- *versus* Second-Generation Products to Secondary Organic Aerosols Formed in the Oxidation of Biogenic Hydrocarbons, *Environ. Sci. Technol.*, 2006, **40**, 2283–2297.

37 D. Stolzenburg, L. Fischer, A. L. Vogel, M. Heinritzi, M. Schervish, M. Simon, A. C. Wagner, L. Dada, L. R. Ahonen, A. Amorim, A. Baccarini, P. S. Bauer, B. Baumgartner, A. Bergen, F. Bianchi, M. Breitenlechner, S. Brilke, S. Buenrostro Mazon, D. Chen, A. Dias, D. C. Draper, J. Duplissy, I. El Haddad, H. Finkenzeller, C. Frege, C. Fuchs, O. Garmash, H. Gordon, X. He, J. Helm, V. Hofbauer, C. R. Hoyle, C. Kim, J. Kirkby, J. Kontkanen, A. Kürten, J. Lampilahti, M. Lawler, K. Lehtipalo, M. Leiminger, H. Mai, S. Mathot, B. Mentler, U. Molteni, W. Nie, T. Nieminen, J. B. Nowak, A. Ojdanic, A. Onnela, M. Passananti, T. Petäjä, L. L. J. Quéléver, M. P. Rissanen, N. Sarnela, S. Schallhart, C. Tauber, A. Tomé, R. Wagner, M. Wang, L. Weitz, D. Wimmer, M. Xiao, C. Yan, P. Ye, Q. Zha, U. Baltensperger, J. Curtius, J. Dommen, R. C. Flagan, M. Kulmala, J. N. Smith, D. R. Worsnop, A. Hansel, N. M. Donahue and P. M. Winkler, Rapid growth of organic aerosol nanoparticles over a wide tropospheric temperature range, *Proc. Natl. Acad. Sci. U. S. A.*, 2018, **115**, 9122–9127.

38 M. Ozon, D. Stolzenburg, L. Dada, A. Seppänen and K. E. J. Lehtinen, Aerosol formation and growth rates from chamber experiments using Kalman smoothing, *Atmos. Chem. Phys.*, 2021, **21**, 12595–12611.

39 M. Glasius, M. Lahaniati, A. Calogirou, D. Di Bella, N. R. Jensen, J. Hjorth, D. Kotzias and B. R. Larsen, Carboxylic Acids in Secondary Aerosols from Oxidation of Cyclic Monoterpenes by Ozone, *Environ. Sci. Technol.*, 2000, **34**, 1001–1010.

40 A. C. Flueckiger and G. A. Petrucci, Methodological advances to improve repeatability of SOA generation in environmental chambers, *Aerosol Sci. Technol.*, 2023, **57**(9), 925–933.

41 K. Kristensen, L. N. Jensen, L. L. J. Quéléver, S. Christiansen, B. Rosati, J. Elm, R. Teiwes,

© 2025 The Author(s). Published by the Royal Society of Chemistry

Environ. Sci.: Atmos., 2025, **5**, 591–602 | **599**

H. B. Pedersen, M. Glasius, M. Ehn and M. Bilde, The Aarhus Chamber Campaign on Highly Oxygenated Organic Molecules and Aerosols (ACCHA): Particle formation, organic acids, and dimer esters from α-pinene ozonolysis at different temperatures, *Atmos. Chem. Phys.*, 2020, **20**, 12549–12567.

42 B. R. Larsen, D. Di Bella, M. Glasius, R. Winterhalter, N. R. Jensen and J. Hjorth, *Gas-phase OH Oxidation of Monoterpenes: Gaseous and Particulate Products*, 2001, vol. 38.

43 W. P. L. Carter, G. Heo, D. R. Cocker III and S. Nakao, *SOA Formation: Chamber Study and Model Development*, Riverside, CA, 2012.

44 C. Song, K. Na and D. R. Cocker, Impact of the Hydrocarbon to NO$_x$ Ratio on Secondary Organic Aerosol Formation, *Environ. Sci. Technol.*, 2005, **39**, 3143–3149.

45 W. C. Porter, J. L. Jimenez and K. C. Barsanti, Quantifying Atmospheric Parameter Ranges for Ambient Secondary Organic Aerosol Formation, *ACS Earth Space Chem.*, 2021, **5**, 2380–2397.

46 X. Ge, A. S. Wexler and S. L. Clegg, Atmospheric amines – Part II. Thermodynamic properties and gas/particle partitioning, *Atmos. Environ.*, 2011, **45**, 561–577.

47 S.-S. Xia, A. J. Eugene and M. I. Guzman, Cross Photoreaction of Glyoxylic and Pyruvic Acids in Model Aqueous Aerosol, *J. Phys. Chem. A*, 2018, **122**, 6457–6466.

48 A. G. Carlton, B. J. Turpin, H. Lim, K. E. Altieri and S. Seitzinger, Link between isoprene and secondary organic aerosol (SOA): Pyruvic acid oxidation yields low volatility organic acids in clouds, *Geophys. Res. Lett.*, 2006, **33**, L06822.

49 Š. Horník, J. Sýkora, P. Pokorná, P. Vodička, J. Schwarz and V. Ždímal, Detailed NMR analysis of water-soluble organic compounds in size-resolved particulate matter seasonally collected at a suburban site in Prague, *Atmos. Environ.*, 2021, **267**, 118757.

50 D. J. Bowden, S. L. Clegg and P. Brimblecombe, The Henry's law constant of trifluoroacetic acid and its partitioning into liquid water in the atmosphere, *Chemosphere*, 1996, **32**, 405–420.

51 L. Bao, M. Matsumoto, T. Kubota, K. Sekiguchi, Q. Wang and K. Sakamoto, Gas/particle partitioning of low-molecular-weight dicarboxylic acids at a suburban site in Saitama, Japan, *Atmos. Environ.*, 2012, **47**, 546–553.

52 T. Yli-Juuti, A. A. Zardini, A. C. Eriksson, A. M. K. Hansen, J. H. Pagels, E. Swietlicki, B. Svenningsson, M. Glasius, D. R. Worsnop, I. Riipinen and M. Bilde, Volatility of organic aerosol: Evaporation of ammonium sulfate/succinic acid aqueous solution droplets, *Environ. Sci. Technol.*, 2013, **47**, 12123–12130.

53 R. Wagner, K. Höhler, O. Möhler, H. Saathoff and M. Schnaiter, Crystallization and immersion freezing ability of oxalic and succinic acid in multicomponent aqueous organic aerosol particles, *Geophys. Res. Lett.*, 2015, **42**, 2464–2472.

54 Y. Y. Zhang, L. Müller, R. Winterhalter, G. K. Moortgat, T. Hoffmann and U. Pöschl, Seasonal cycle and temperature dependence of pinene oxidation products, dicarboxylic acids and nitrophenols in fine and coarse air particulate matter, *Atmos. Chem. Phys.*, 2010, **10**, 7859–7873.

55 L. Müller, M.-C. Reinnig, K. H. Naumann, H. Saathoff, T. F. Mentel, N. M. Donahue and T. Hoffmann, Formation of 3-methyl-1,2,3-butanetricarboxylic acid *via* gas phase oxidation of pinonic acid – a mass spectrometric study of SOA aging, *Atmos. Chem. Phys.*, 2012, **12**, 1483–1496.

56 L. Wu, C. Becote, S. Sobanska, P.-M. Flaud, E. Perraudin, E. Villenave, Y.-C. Song and C.-U. Ro, Hygroscopic behavior of aerosols generated from solutions of 3-methyl-1,2,3-butanetricarboxylic acid, its sodium salts, and its mixtures with NaCl, *Atmos. Chem. Phys.*, 2020, **20**, 14103–14122.

57 M. Brüggemann, R. Xu, A. Tilgner, K. C. Kwong, A. Mutzel, H. Y. Poon, T. Otto, T. Schaefer, L. Poulain, M. N. Chan and H. Herrmann, Organosulfates in Ambient Aerosol: State of Knowledge and Future Research Directions on Formation, Abundance, Fate, and Importance, *Environ. Sci. Technol.*, 2020, **54**, 3767–3782.

58 A. M. Fankhauser, Z. Lei, K. R. Daley, Y. Xiao, Z. Zhang, A. Gold, B. S. Ault, J. D. Surratt and A. P. Ault, Acidity-Dependent Atmospheric Organosulfate Structures and Spectra: Exploration of Protonation State Effects *via* Raman and Infrared Spectroscopies Combined with Density Functional Theory, *J. Phys. Chem. A*, 2022, **126**, 5974–5984.

59 A. Bain, M. N. Chan and B. R. Bzdek, Physical properties of short chain aqueous organosulfate aerosol, *Environ. Sci.: Atmos.*, 2023, **3**, 1365–1373.

60 *CRC Handbook of Chemistry and Physics*, ed. J. R. Rumble, CRC Press/Taylor & Francis, Boca Raton, FL, 104th edn, 2023.

61 E. Wilhelm, R. Battino and R. J. Wilcock, Low-pressure solubility of gases in liquid water, *Chem. Rev.*, 1977, **77**, 219–262.

62 *NIST Chemistry WebBook, NIST Standard Reference Database Number 69*, ed. P. J. Linstrom and W. G. Mallard, National Institute of Standards and Technology, Gaithersburg, MD, retrieved July 15, 2024.

63 P. Bénézeth, D. A. Palmer and D. J. Wesolowski, Potentiometric Study of the Dissociation Quotients of Aqueous Dimethylammonium Ion As a Function of Temperature and Ionic Strength, *J. Chem. Eng. Data*, 2001, **46**, 202–207.

64 M. Darji, A. Manhas, S. K. Dash and K. Mukherjee, Dissociation Constants of Amine Solvents Used in CO$_2$ Capture: Titrimetric Estimation and Density Functional Theory Calculation, *Ind. Eng. Chem. Res.*, 2023, **62**, 7868–7876.

65 R. Bone, P. Cullis and R. Wolfenden, Solvent effects on equilibria of addition of nucleophiles to acetaldehyde and the hydrophilic character of diols, *J. Am. Chem. Soc.*, 1983, **105**, 1339–1343.

66 Dortmund Data Bank, https://www.ddbst.com/.

67 A. V. Rayer and A. Henni, Heats of Absorption of CO2 in Aqueous Solutions of Tertiary Amines: N-Methyldiethanolamine, 3-Dimethylamino-1-propanol, and 1-Dimethylamino-2-propanol, *Ind. Eng. Chem. Res.*, 2014, **53**, 4953–4965.

68 S. Ma'mun, S. Kamariah, D. Kurniawan, E. Amelia, V. Rahmat and D. R. Alwani, Experimental determination of monoethanolamine protonation constant and its temperature dependency, *MATEC Web Conf.*, 2017, **101**, 02001.

69 Y. Wei, T. Cao and J. E. Thompson, The chemical evolution & physical properties of organic aerosol: A molecular structure based approach, *Atmos. Environ.*, 2012, **62**, 199–207.

70 Y.-J. Jin and G. Kwak, Detection of biogenic amines using a nitrated conjugated polymer, *Sens. Actuators, B*, 2018, **271**, 183–188.

71 J. A. Brown, Haz-Map, Information on Hazardous Chemicals and Occupational Diseases, **https://haz-map.com/**, accessed 14 October 2024.

72 HSDB: Hazardous Substances Data Bank, TOXicology data NET-work (TOXNET), **https://www.nlm.nih.gov/toxnet/index.html**, accessed 14 October 2024.

73 J. L. Kurz and J. M. Farrar, Entropies of dissociation of some moderately strong acids, *J. Am. Chem. Soc.*, 1969, **91**, 6057–6062.

74 S. Kutsuna and H. Hori, Experimental determination of Henry's law constants of trifluoroacetic acid at 278–298K, *Atmos. Environ.*, 2008, **42**, 1399–1412.

75 P. Thakur, J. N. Mathur, R. C. Moore and G. R. Choppin, Thermodynamics and dissociation constants of carboxylic acids at high ionic strength and temperature, *Inorg. Chim. Acta*, 2007, **360**, 3671–3680.

76 S. L. Clegg, P. Brimblecombe and I. Khan, The Henry's Law constant of oxalic acid and its partitioning into the atmospheric aerosol, *Idojaras*, 1996, **100**, 51–68.

77 V. Soonsin, A. A. Zardini, C. Marcolli, A. Zuend and U. K. Krieger, The vapor pressures and activities of dicarboxylic acids reconsidered: the impact of the physical state of the aerosol, *Atmos. Chem. Phys.*, 2010, **10**, 11753–11767.

78 S. Compernolle and J.-F. Müller, Henry's law constants of diacids and hydroxy polyacids: recommended values, *Atmos. Chem. Phys.*, 2014, **14**, 2699–2712.

79 P. Brimblecombe, S. L. Clegg and I. Khan, Thermodynamic properties of carboxylic acids relevant to their solubility in aqueous solutions, *J. Aerosol Sci.*, 1992, **23**, 901–904.

80 G. El-Naggar, First and second dissociation constants and related thermodynamic functions of adipic acid in various binary methanol/solvent systems, *Talanta*, 1998, **47**, 1013–1020.

81 M. Bilde, B. Svenningsson, J. Mønster and T. Rosenørn, Even–Odd Alternation of Evaporation Rates and Vapor Pressures of C3–C9 Dicarboxylic Acid Aerosols, *Environ. Sci. Technol.*, 2003, **37**, 1371–1378.

82 L. A. Ashton and J. I. Bullock, Effect of temperature on the ionisation constants of 2-, 3- and 4-nitrobenzoic, phthalic

83 and nicotinic acids in aqueous solution, *J. Chem. Soc., Faraday Trans.*, 1982, **78**, 1177.

83 K. Chatterjee, A. Hazra, D. Dollimore and K. S. Alexander, An Evaporation Study for Phthalic Acids—A Rapid Method for Pharmaceutical Characterization, *J. Pharm. Sci.*, 2002, **91**, 1156–1168.

84 F. D. Pope, H.-J. Tong, B. J. Dennis-Smither, P. T. Griffiths, S. L. Clegg, J. P. Reid and R. A. Cox, Studies of Single Aerosol Particles Containing Malonic Acid, Glutaric Acid, and Their Mixtures with Sodium Chloride. II. Liquid-State Vapor Pressures of the Acids, *J. Phys. Chem. A*, 2010, **114**, 10156–10165.

85 T. Hirokawa, in *Capillary Electromigration Separation Methods*, Elsevier, 2018, pp. 189–208.

86 I. Khan, P. Brimblecombe and S. L. Clegg, Solubilities of Pyruvic Acid and the Lower (C1-C6) Carboxylic Acids, *Experimental Determination of Equilibrium Vapour Pressures above Pure Aqueous and Salt Solutions*, Kluwer Academic Publishers, 1995, vol. 22.

87 V. N. Emel'yanenko, V. V. Turovtsev and Y. A. Fedina, Thermodynamic properties of pyruvic acid and its methyl ester, *Thermochim. Acta*, 2018, **665**, 70–75.

88 A. Kołodziejczyk, A. Wróblewska, M. Pietrzak, P. Pyrcz, K. Błaziak and R. Szmigielski, Dissociation constants of relevant secondary organic aerosol components in the atmosphere, *Chemosphere*, 2024, **351**, 141166.

89 M. Bilde and S. N. Pandis, Evaporation Rates and Vapor Pressures of Individual Aerosol Species Formed in the Atmospheric Oxidation of α- and β-Pinene, *Environ. Sci. Technol.*, 2001, **35**, 3344–3349.

90 H. Howell, G. S. Fisher and B. Hilda Howell, *Depart-ment of Agriculture*, ed. W. Dieckmann and Albín Hardt, 1958, vol. 19.

91 A. Kołodziejczyk, P. Pyrcz, A. Pobudkowska, K. Błaziak and R. Szmigielski, Physicochemical Properties of Pinic, Pinonic, Norpinic, and Norpinonic Acids as Relevant α-Pinene Oxidation Products, *J. Phys. Chem. B*, 2019, **123**, 8261–8267.

92 R. N. Goldberg, N. Kishore and R. M. Lennen, Thermodynamic Quantities for the Ionization Reactions of Buffers, *J. Phys. Chem. Ref. Data*, 2002, **31**, 231–370.

93 H. D. Belitz, W. Grosch and P. Schieberle, *Food Chemistry 4th Revised and Extended Edition*, 2009, vol. 53.

94 V. N. Emel'yanenko, S. P. Verevkin, C. Schick, E. N. Stepurko, G. N. Roganov and M. K. Georgieva, The thermodynamic properties of S-lactic acid, *Russ. J. Phys. Chem. A*, 2010, **84**, 1491–1497.

95 *Biotechnology of Yeasts and Filamentous Fungi*, ed. A. A. Sibirny, Springer International Publishing, Cham, 2017.

96 S. P. Verevkin and V. N. Emel'yanenko, Renewable platform-chemicals and materials: Thermochemical study of levulinic acid, *J. Chem. Thermodyn.*, 2012, **46**, 94–98.

97 J. S. Chickos and W. E. Acree, Enthalpies of Vaporization of Organic and Organometallic Compounds, 1880–2002, *J. Phys. Chem. Ref. Data*, 2003, **32**, 519–878.

© 2025 The Author(s). Published by the Royal Society of Chemistry

Environ. Sci.: Atmos., 2025, **5**, 591–602 | 601

98 H. S. Simon Ip, X. H. H. Huang and J. Z. Yu, Effective Henry's law constants of glyoxal, glyoxylic acid, and glycolic acid, *Geophys. Res. Lett.*, 2009, **36**, L01802.

99 D. M. Lienhard, A. J. Huisman, U. K. Krieger, Y. Rudich, C. Marcolli, B. P. Luo, D. L. Bones, J. P. Reid, A. T. Lambe, M. R. Canagaratna, P. Davidovits, T. B. Onasch, D. R. Worsnop, S. S. Steimer, T. Koop and T. Peter, Viscous organic aerosol particles in the upper troposphere: diffusivity-controlled water uptake and ice nucleation?, *Atmos. Chem. Phys.*, 2015, **15**, 13599–13613.

100 S. H. Hilal, S. W. Karickhoff and L. A. Carreira, Prediction of the Solubility, Activity Coefficient and Liquid/Liquid Partition Coefficient of Organic Compounds, *QSAR Comb. Sci.*, 2004, **23**, 709–720.

101 G. Olofsson, Thermodynamic quantities for the dissociation of the ammonium ion and for the ionization of aqueous ammonia over a wide temperature range, *J. Chem. Thermodyn.*, 1975, **7**, 507–514.

102 H. Dai, J. Zhang, H. Gui, L. Shen, X. Wei, Z. Xie, S. Chen, Z. Wu, D.-R. Chen and J. Liu, Characteristics of aerosol size distribution and liquid water content under ambient RH conditions in Beijing, *Atmos. Environ.*, 2022, **291**, 119397.

103 A. Yazdani, A. M. Dillner and S. Takahama, Estimating mean molecular weight, carbon number, and OM/OC with mid-infrared spectroscopy in organic particulate matter samples from a monitoring network, *Atmos. Meas. Tech.*, 2021, **14**, 4805–4827.

104 W. Zhang, G. Xu, B. Xi, J. Ren, X. Wan, L. Zhou, C. Cui and D. Wu, Comparative Study of Cloud Liquid Water and Rain Liquid Water Obtained From Microwave Radiometer and Micro Rain Radar Observations Over Central China During the Monsoon, *J. Geophys. Res.:Atmos.*, 2020, **125**(20), e2020JD032456.

105 J. J. Schauer, M. J. Kleeman, G. R. Cass and B. R. T. Simoneit, Measurement of Emissions from Air Pollution Sources. 2. C_1 through C_{30} Organic Compounds from Medium Duty Diesel Trucks, *Environ. Sci. Technol.*, 1999, **33**, 1578–1587.

106 B. R. T. Simoneit, J. N. Cardoso and N. Robinson, An assessment of the origin and composition of higher molecular weight organic matter in aerosols over Amazonia, *Chemosphere*, 1990, **21**, 1285–1301.

107 R. E. Skyner, J. L. McDonagh, C. R. Groom, T. van Mourik and J. B. O. Mitchell, A review of methods for the calculation of solution free energies and the modelling of systems in solution, *Phys. Chem. Chem. Phys.*, 2015, **17**, 6174–6191.

108 B. Hess and N. F. A. van der Vegt, Hydration Thermodynamic Properties of Amino Acid Analogues: A Systematic Comparison of Biomolecular Force Fields and Water Models, *J. Phys. Chem. B*, 2006, **110**, 17616–17626.

109 G. Duarte Ramos Matos, D. Y. Kyu, H. H. Loeffler, J. D. Chodera, M. R. Shirts and D. L. Mobley, Approaches for Calculating Solvation Free Energies and Enthalpies Demonstrated with an Update of the FreeSolv Database, *J. Chem. Eng. Data*, 2017, **62**, 1559–1569.